The Plant Cell, Vol. 9, 689–701, May 1997 © 1997 American Society of Plant Physiologists

Collapsed Xylem Phenotype of Arabidopsis Identifies Mutants Deficient in Cellulose Deposition in the Secondary Cell Wall

Simon R. Turner[a,1] and Chris R. Somerville[b]

[a]University of Manchester, School of Biological Science, 3.614 Stopford Building, Oxford Road, Manchester M13 9PT, United Kingdom

[b]Department of Plant Biology, Carnegie Institution of Washington, 290 Panama Street, Stanford, California 94305

Recessive mutations at three loci cause the collapse of mature xylem cells in inflorescence stems of Arabidopsis. These irregular xylem (*irx*) mutations were identified by screening plants from a mutagenized population by microscopic examination of stem sections. The xylem cell defect was associated with an up to eightfold reduction in the total amount of cellulose in mature inflorescence stems. The amounts of cell wall–associated phenolics and polysaccharides were unaffected by the mutations. Examination of the cell walls by using electron microscopy demonstrated that the decreases in cellulose content of *irx* lines resulted in an alteration of the spatial organization of cell wall material. This suggests that a normal pattern of cellulose deposition may be required for assembly of lignin or polysaccharides. The reduced cellulose content of the stems also resulted in a decrease in stiffness of the stem material. This is consistent with the irregular xylem phenotype and suggests that the walls of *irx* plants are not resistant to compressive forces. Because lignin was implicated previously as a major factor in resistance to compressive forces, these results suggest either that cellulose has a direct role in providing resistance to compressive forces or that it is required for the development of normal lignin structure. The *irx* plants had a slight reduction in growth rate and stature but were otherwise normal in appearance. The mutations should be useful in facilitating the identification of factors that control the synthesis and deposition of cellulose and other cell wall components.

INTRODUCTION

Much of what is currently known about the structure of plant cell walls has been inferred from attempts to correlate microscopic images with structural studies of the principal extractable components (McCann et al., 1995). This combination of approaches has revealed the general principles of the organization of wall components and permitted the development of several useful working models (Carpita and Gibeaut, 1993; McCann and Roberts, 1994). However, relatively little is known concerning the higher order structure of the wall and the contribution that individual components make to the physical properties and functions of the wall. Also, virtually nothing is known about the enzymes that catalyze synthesis of the polysaccharide components of cell walls. None of the enzymes associated with the synthesis of cellulose, xyloglucan, xylan, callose, or the pectic polysaccharides has yet been isolated (Delmer and Amor, 1995). The recent identification of candidate genes for cellulose synthase by genomic methods represents the first step toward determining which genes might be directly involved in the synthesis of a cell wall polysaccharide (Pear et al., 1996). Similarly, although the pathway for the biosynthesis of monolignols, the monomers required for lignin synthesis, is relatively well understood, many questions about the structure and formation of lignin remain (reviewed in Lewis and Yamamoto, 1990; Whetten and Sederoff, 1995). For example, we do not know whether the polymerization of monolignols is catalyzed by a peroxidase or a laccase and to what extent lignin is a randomly formed structure. In addition to cellulose and lignin, there are many other cell wall components, and the roles that they play in determining both the properties of the cell wall and its proper assembly remain largely unknown (Carpita and Gibeaut, 1993; McCann and Roberts, 1994).

Genetic methods have rarely been applied to the general problem of cell wall polysaccharide structure and function (reviewed in Reiter, 1994). Among the few mutants known to affect the polysaccharide component of cell walls are the *brittle culm* mutants of maize, rice, and barley. The barley lines have a reduction in the amount of cellulose in the cell wall to ~20% of that in the wild type, and the walls exhibit a twofold decrease in breaking strength (Kokubo et al., 1989, 1991). The biochemical basis for the defect in the *brittle culm* mutants has not been determined. Mutants of Arabidopsis

[1]To whom correspondence should be addressed. E-mail simon.turner@man.ac.uk; fax 44-161-275-3938.

with altered polysaccharide composition have been identified by direct analysis of the total monosaccharide composition of leaf cell walls (Reiter et al., 1993). Mutations at 12 different loci were recovered by using this approach, but the enzymatic defect has been characterized for only one mutant, a line deficient in fucose synthesis (W.-D. Reiter, C.S. Chapple, and C.R. Somerville, unpublished data).

An Arabidopsis mutant with altered cellulose deposition in the secondary cell walls of trichomes was identified by screening for the altered appearance of trichomes under polarized light (Potika and Delmer, 1995). The apparent cell-type specificity of this mutant has prevented a detailed examination for the basis of this defect. Although the enzymatic defects in most of the Arabidopsis mutants are not yet known, it is expected that the sequencing of the entire Arabidopsis genome will greatly facilitate the identification of the corresponding genes (Somerville and Somerville, 1996). Thus, it is an opportune time to expand the collection of mutants that specifically alter the structure and function of the cell wall. In anticipation of this opportunity, a detailed characterization of the composition of Arabidopsis cell walls has shown that they are typical of many higher plants (Zablackis et al., 1995).

The differentiation of tracheary elements, the large water-conducting cells of the xylem, has been extensively used as a model for plant cell differentiation and secondary wall deposition (reviewed in Fukada, 1992). These xylem elements are highly specialized for carrying water and solute throughout the plant. At maturity, the xylem elements die and lose their cell contents. This process allows relatively unimpeded water flow through the xylem. Although controversy still exists as to the exact mechanism of water transport in plants, all models agree that the process of carrying water from the roots to the leaves, where it is lost due to transpiration, generates a negative pressure in the xylem (Zimmerman et al., 1994; Shackel, 1996). This negative pressure causes a large compressive force to be placed on tracheary elements of the xylem. To prevent their collapse, the walls of these cells are strengthened by an elaborate pattern of secondary cell wall thickening, which includes the deposition of cellulose and lignin (Raven, 1977). The consequences of disrupting secondary cell wall formation were demonstrated by experiments in which lignin synthesis was inhibited. Bean seedlings grown in the presence of a phenylalanine ammonia-lyase inhibitor exhibited greatly reduced lignin content in the walls of the xylem elements (Amrhein et al., 1983; Smart and Amrhein, 1985). As a result, the xylem cells were no longer able to maintain a fully expanded shape and collapsed inward.

Here, we describe three novel mutants of Arabidopsis in which the walls of the mature xylem elements appear to spontaneously collapse inward. These mutants all have greatly reduced cellulose content in secondary cell walls. This decrease in cellulose is correlated with alterations in the physical properties of the wall and consequently offers some insight into the role of cellulose in determining the properties of the secondary cell wall.

RESULTS

Xylem Development in Arabidopsis Stems

The organization of vascular tissue in mature inflorescence stems of Arabidopsis can be conveniently visualized in hand-cut sections stained with toluidine blue (Figure 1). In Arabidopsis, the xylem cells typically are confined to six to eight discrete vascular bundles that are separated by the sclerified parenchyma of the interfascicular region. Xylem elements die at maturity and lose their cell contents. Consequently, they may be easily identified as large round empty-looking cells with relatively thick uniform cell walls (Figures 1 and 2E). In the mature stems, cells from both the interfascicular region and the xylem have thick, lignified secondary cell walls. Toluidine blue staining showed that these walls form a continuous ring around the stem (Figures 1 and 2E).

During the process of stem maturation in Arabidopsis, the xylem elements arise from the cells of the procambium. The cell divisions that give rise to the cells of the procambium occur close to the apical meristem. The xylem elements are formed by the differentiation of these procambial cells. This developmental process involves the early protoxylem elements forming close to the top of the stem and toward the inside of the vascular bundle (Figure 2A). In older tissue, farther down the stem, the later metaxylem elements differentiate toward the outside of the stem, adjacent to the phloem (Figures 2C and 2E). In mature tissue, few procambial cells remain, and the vascular bundle is composed almost exclusively of xylem and phloem (Figure 2E). One consequence of this sequential developmental progression is that it is possible to monitor xylem development in a single Arabidopsis stem simply by sectioning at different distances from the apical meristem.

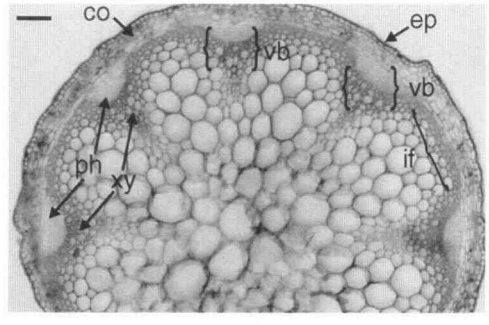

Figure 1. Transverse Section of a Wild-Type Arabidopsis Stem Stained with Toluidine Blue.

Vascular bundles (vb), xylem (xy), phloem (ph), cortex (co), epidermis (ep), and the interfascicular region (if) are indicated. Bar = 0.1 mm.

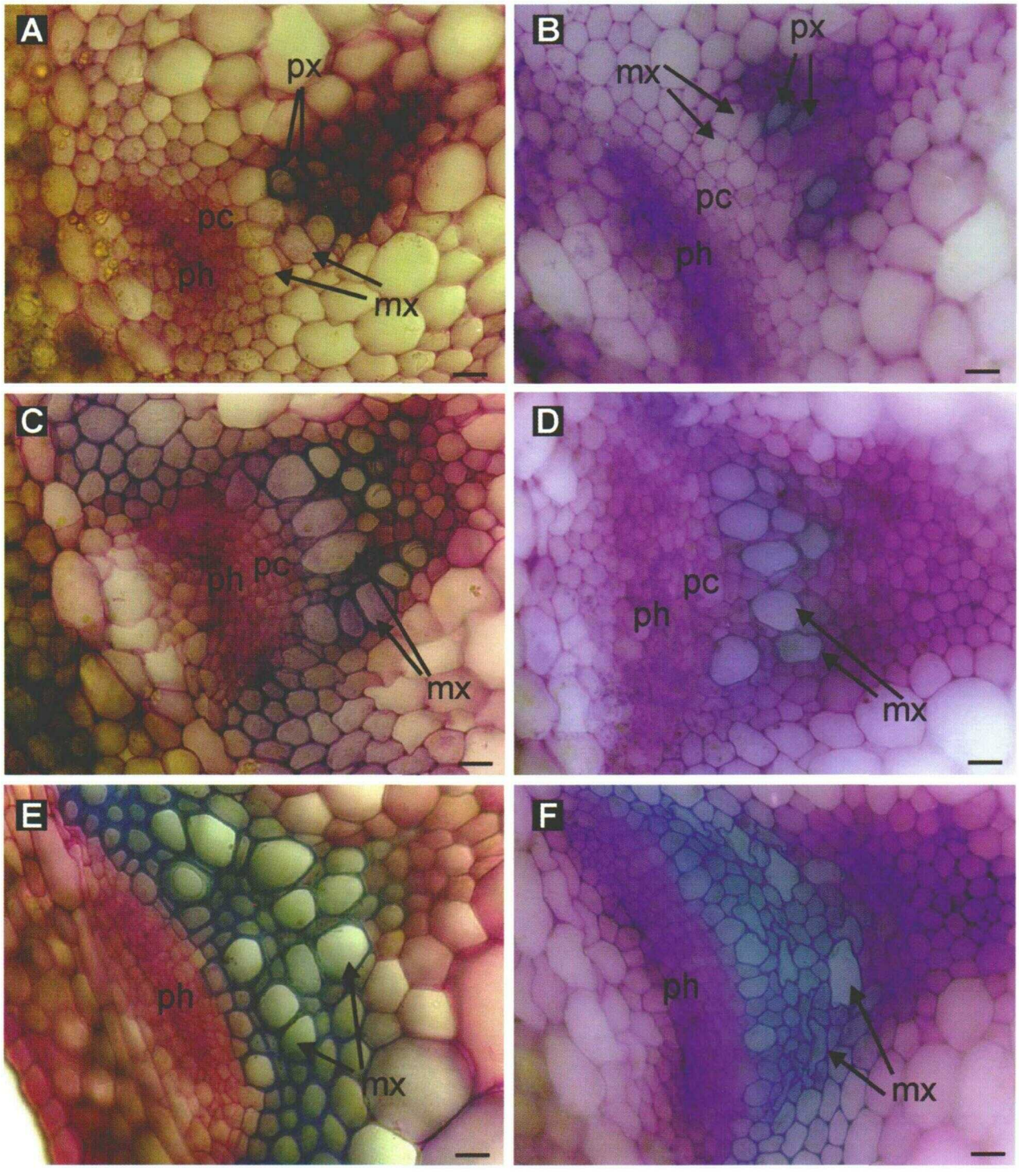

Figure 2. Xylem Element Differentiation during Inflorescence Stem Development.

Transverse stem sections stained with toluidine blue were taken from various points of a single wild-type or *irx1* stem. A single representative vascular bundle from each section is shown. The protoxylem (px), metaxylem (mx), procambium (pc), and phloem (ph) are indicated.
(A), **(C)**, and **(E)** From the top, middle, and base of a wild-type stem, respectively.
(B), **(D)**, and **(F)** From the top, middle, and base of an *irx1* stem, respectively.
Bars = 12.5 μm.

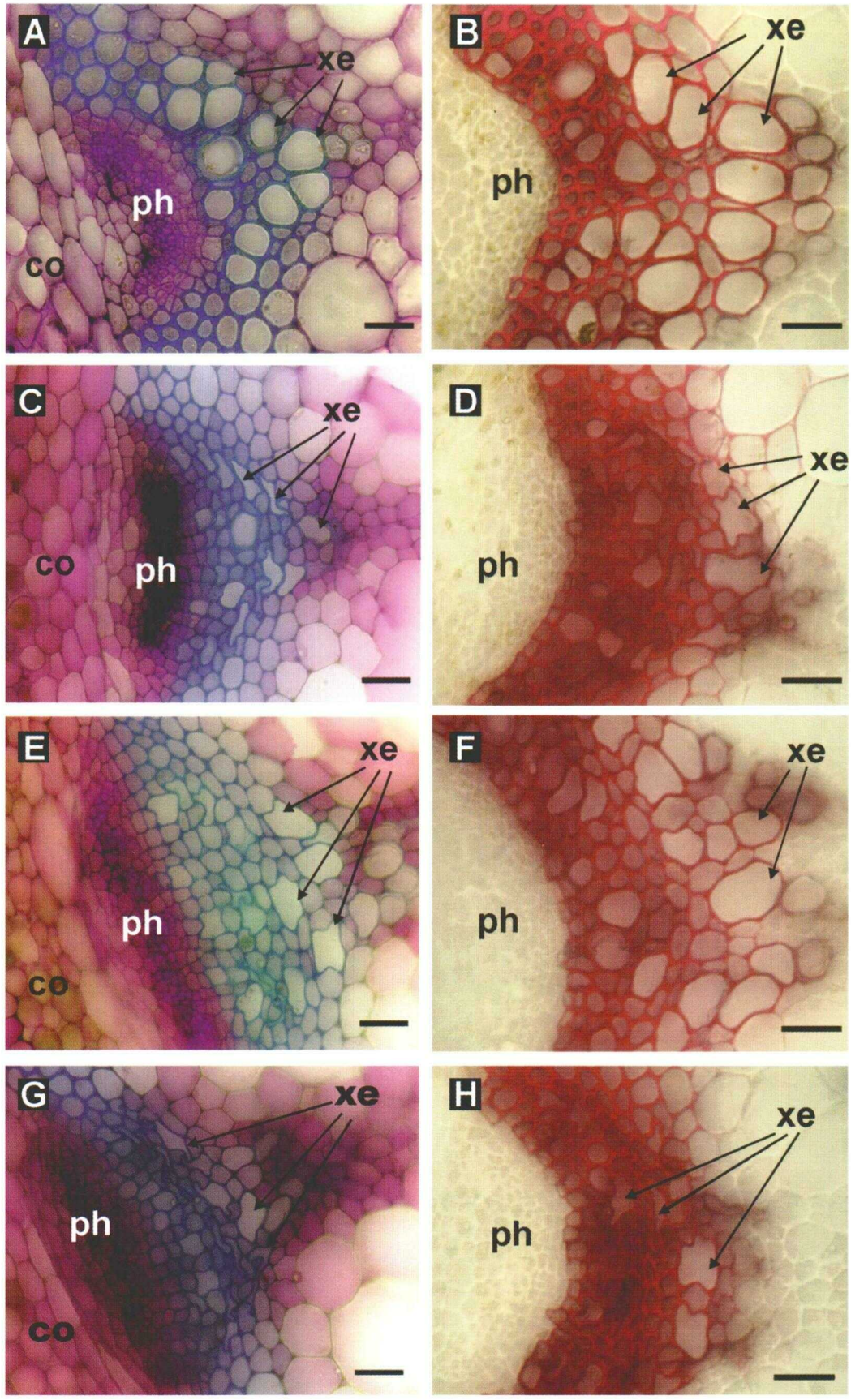

Figure 3. Cross-Sections of Stem Vascular Bundles from Wild-Type and *irx* Plants.

Mutant Isolation and Genetic Analysis

Randomly chosen M_2 plants (~1600) from several independent ethyl methanesulfonate–mutagenized populations were screened for altered xylem cell morphology by examining hand-cut stem sections that were stained with toluidine blue, using light microscopy. In addition, ~4600 plants were prescreened for stem strength by using subjective tests to determine the relative effort required to break a stem by hand. The organization and structure of the vascular tissue in 100 of these prescreened plants were then examined by sectioning the stem.

Eight lines were isolated in which the vascular tissue contained irregular, collapsed-looking xylem elements (Figure 3). Five of these lines were from the unselected population, and three were recovered from the 100 prescreened plants. Mutants that exhibited collapsed xylem elements when viewed in cross-section were named irregular xylem (*irx*) mutants. Complementation analysis was performed by making reciprocal crosses between the mutants and scoring six to 20 F_1 progeny from each cross by using light microscopy of stem sections. Three lines (SRT123 [*irx1*], SRT228 [*irx2-1*], and SRT206 [*irx3*]) from a Landsberg *erecta* background and one line from a Columbia background (SRT177 [*irx2-2*]) were retained as carrying independent alleles representing three complementation groups. The other four lines, which also carried mutant alleles of the three *irx* loci, were not studied further because we could not verify that they were independent alleles.

Crosses were made between a representative from each of the three *irx* complementation groups and wild-type line M53, and the segregation of the irregular xylem phenotype was scored in the F_2 generation. The SRT123 (*irx1*) × M53 cross gave 219 wild-type and 67 *irx* plants, which is an excellent fit to the 3:1 hypothesis (χ^2 = 0.3; P = 0.584). Similarly, SRT228-1 (*irx2*) × M53 gave 206 wild-type and 58 *irx* plants [χ^2 (3:1) = 1.29; P = 0.26], and SRT206 (*irx3*) × M53 gave 55 wild-type and 24 *irx* plants [χ^2 (3:1) = 1.07; P = 0.3]. Thus, all three *irx* mutations segregated as single nuclear recessive mutations.

Progeny from the F_2 generation of the SRT206 (*irx3*) × M53 cross were scored with a number of polymerase chain reaction–based markers to place the *irx3* mutation on the genetic map of Arabidopsis. The *irx3* locus showed linkage to microsatellite markers nga249, nga151, nga106, and nga139. A map calculated by using three-point linkage analysis (Lander et al., 1987) is shown in Figure 4. This map, which is in good agreement with that described by Bell and Ecker (1994), places the *irx3* mutation in the middle of chromosome 5 close to the marker nga106.

Mutant Phenotype

With the exception of the collapsed xylem phenotype, both the organization of the vascular tissue and the organization of the entire stem of the three *irx* mutants are identical to that of the wild type (Figure 1). In addition to stems, the collapsed xylem phenotype of *irx* plants has been observed in mature hypocotyls and in the primary root and petioles (data not shown). The developmental progression of the *irx* mutant syndrome, which was indistinguishable in the three mutant classes, is shown for the *irx1* mutant in Figures 2B, 2D, and 2F. During the course of vascular development in the *irx* mutants, the xylem elements initially appear to expand correctly and to attain their normal shape (Figure 2B). Even in xylem elements that appear to be almost mature, in which some cell wall deposition has occurred, most of the cells appear to have a normal shape (Figure 2D). Only in sections from mature stems in which the xylem elements are mature, and presumably actively involved in the transport of water, is the collapsed xylem phenotype of the *irx* mutants most obvious (Figure 2F).

In general, *irx* plants grow normally and do not exhibit any readily apparent alterations in morphology, except that *irx* mutants are slightly smaller than the wild type (Figure 5). In addition, *irx1* and *irx3* plants tend to grow slightly more slowly than do wild type plants. One interesting phenotype

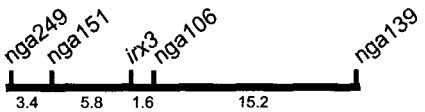

Figure 4. Map Position of *irx3* on Chromosome 5 Relative to Several Microsatellite Markers.

Values below the line are the genetic distances in centimorgans between adjacent markers, as calculated by Mapmaker 3.0.

Figure 3. (continued).

Sections were stained with toluidine blue (**[A]**, **[C]**, **[E]**, and **[G]**) or phloroglucinol (**[B]**, **[D]**, **[F]**, and **[H]**). The cortex (co), phloem (ph), and xylem elements (xe) are indicated.
(A) and **(B)** Wild type.
(C) and **(D)** *irx1*.
(E) and **(F)** *irx2*.
(G) and **(H)** *irx3*.
Bars = 25 μm.

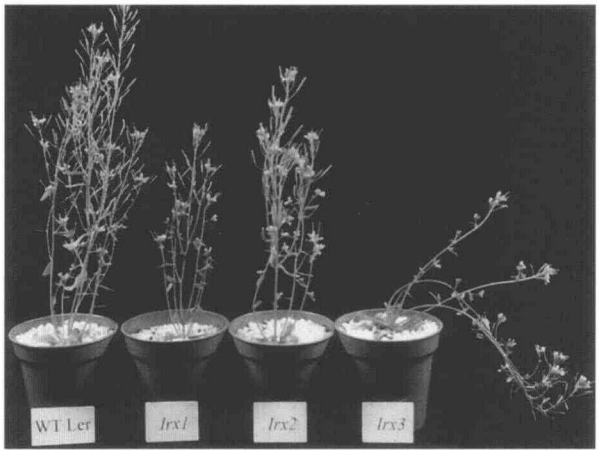

Figure 5. Mature Plants of Landsberg *erecta* and the *irx* Mutant Lines.

WT Ler, wild-type Landsberg *erecta*.

exhibited by *irx3* plants concerns the properties of the inflorescence stems. Stems of *irx3* plants are less rigid than those of the wild type and tend to recline, which is in contrast to the upright growth habit of wild-type stems (Figure 5). None of the *irx* plants exhibited any obvious increase in their susceptibility to wilting.

Ultrastructure

On the basis of light microscopic examination of collapsed xylem elements, it is unclear whether the alterations in the appearance of the cell wall contributed to the collapse of the element or whether the alterations occurred as a result of the collapse. Consequently, the interpretation of alterations in the appearance of xylem cell walls is complicated by uncertainty about cause and effect. In contrast, walls from the heavily thickened cells of the interfascicular region showed no evidence of collapse (Figures 1, 3A, and 3B) and exhibited a relatively even pattern of cell wall thickening.

To examine the cell wall structure in detail, stem sections from the interfascicular region were examined by using transmission electron microscopy. The cell walls from the in-

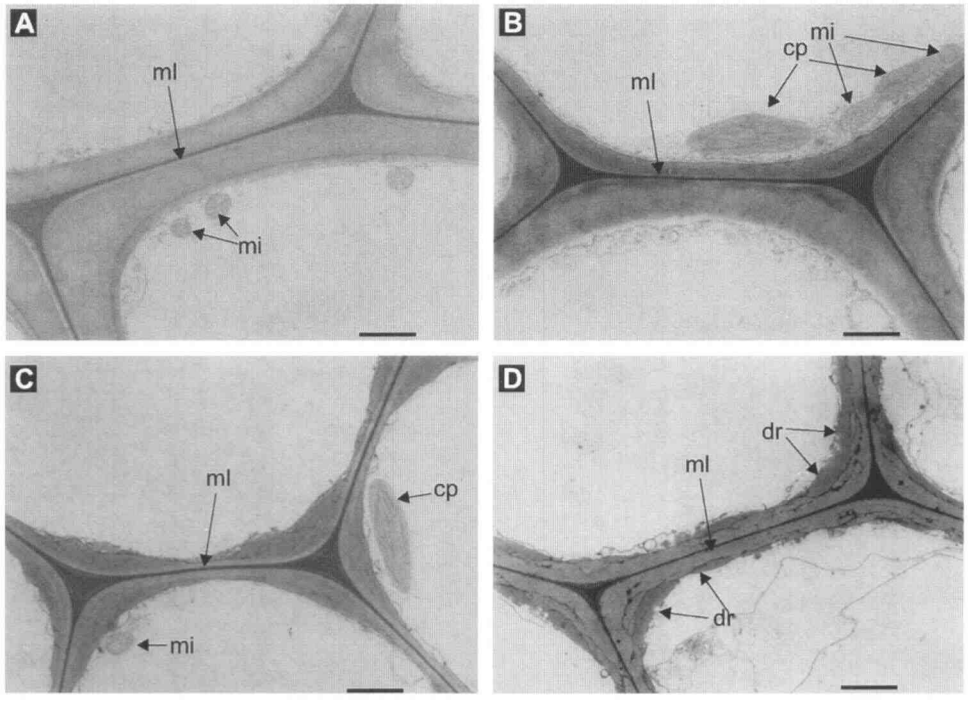

Figure 6. Transmission Electron Microscopy of Cell Walls from the Interfascicular Region of Mature Stems from Wild-Type and *irx* Plants.

The mid-lamellae (ml) region is easily distinguishable as the very dark staining region in the center of the walls. Mitochondria (mi), chloroplasts (cp), and a darker staining outer region (dr) are also indicated.
(A) Stem from a wild-type plant.
(B) to **(D)** Stems from *irx1*, *irx2*, and *irx3* plants, respectively.
Bars = 1.5 μm.

terfascicular region of wild-type plants are generally of similar thickness around the entire cell and appear to stain in a ubiquitous manner (Figure 6A). The walls from *irx1* plants are similar in appearance to the wild type but are slightly thinner than those of the wild type (Figure 6B). In contrast to the even pattern of thickening seen in the wild type, the walls of *irx2* plants show a preferential deposition of cell wall material in the corners of the cells (Figure 6C). There is a pronounced decrease in the width of the walls at the midpoint of the wall. Although the bulk of the walls of the *irx2* mutant stain in a fairly ubiquitous manner, thin darker staining lines were observed that appear to break up the wall into different domains (Figure 6C). The walls from *irx3* plants also appear to show different domains, with a darker staining outer region (designated *or*) attached to the sides (Figure 6D). In general, the walls of *irx3* plants appear to show a very uneven pattern of cell wall deposition compared with that of the wild type (Figure 6D).

Physical Properties of *irx* Plant Stems

In addition to the altered growth habit of *irx3* (Figure 5), subjective evaluations indicated that all three mutants appeared to have weak stems. To quantify the physical properties of stems, we conducted three-point bending tests with stem segments from wild-type and *irx* plants. Maximum stress at yield was used as a measure of the strength of the stem material. The stiffness of the stem material is indicated by the bending modulus, a material property derived from the initial force required to bend the stem segment. A higher bending modulus indicates stiffer material.

The results of these measurements on wild-type and *irx* stems during the course of stem maturation are shown in Figure 7. The largest differences were observed in the stiffness (bending modulus) of the stem material. In 48-day-old plants, the bending modulus of *irx3* is only 10% that of the wild type (Figure 7A). In addition, smaller but significant differences were observed in the maximum stress at yield between wild-type and that of *irx2* and *irx3* plants (Figure 7B). For both the bending modulus and the maximum stress at yield, the differences between wild-type and *irx* plants became greater with increasing stem age. For example, between 34 and 48 days, the bending modulus of *irx1* decreased from 48 to 34% that of the wild-type value, and the maximum load at yield of *irx2* dropped from 82 to 65% that of the wild-type value.

At all stages of development, both the bending modulus and maximum stress at yield of *irx1* were always closest to the wild-type value. *Irx3* always exhibited the greatest changes in both physical properties. However, not all of the mutations affected the two physical properties in the same way. For example, in stems from 34-day-old plants, the maximum stress at yield for *irx2* and *irx3* was similar, whereas the bending modulus of *irx3* was less than half that of *irx2*. When we compare the effects of *irx2* and *irx3* on the physical properties of the stem material, it may be seen that the *irx3* mutation has a greater effect on stiffness than it does on strength at all stages of development. It is presumably the low stiffness of the *irx3* stem material that is the cause of the plant's apparent inability to support an upright growth habit (Figure 5).

Lignin Analysis

Because the *irx* phenotype resembles that of plants with reduced lignin (Smart and Amrhein, 1985), initial efforts to determine the nature of the biochemical defect in the walls of *irx* plants focused on the lignin fraction of the wall. In the wild type, the walls of xylem cells stain a bright red when phloroglucinol is used. All three *irx* mutants showed a positive reaction with phloroglucinol in a manner similar to the wild type (Figures 3D, 3F, and 3H). Little or no difference was detected in either the color or the distribution of the positively stained material. No detectable differences were observed with other stains, such as aniline sulfate, which is considered diagnostic for lignin (data not shown). A comparison of the blue color of lignified cell walls stained with toluidine blue (Figures 3A, 3C, 3E, and 3G) revealed no difference between the wild type and *irx* mutants. Based on this histochemical evidence, it was concluded that there were no apparent qualitative alterations in the deposition of lignin in *irx* plants.

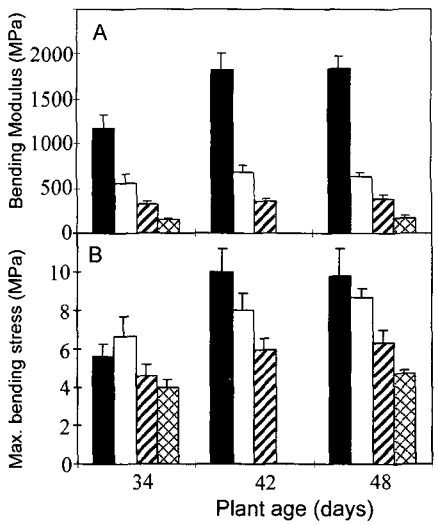

Figure 7. Physical Properties of Stems from Wild-Type and *irx* Plants.

Measurements were conducted with stem segments from wild-type (solid bars), *irx1* (open bars), *irx2* (hatched bars), and *irx3* (cross-hatched bars) plants at three stages of development. Standard error bars are shown ($n > 10$).

(A) The bending modulus.

(B) Maximum stress at yield.

Table 1. Percentage of Total Phenolic Content of an Ethanol-Insoluble Cell Wall Fraction

Line	Total Phenolics[a] (%)
Landsberg *erecta*	8.12 ± 0.13
irx1	9.33 ± 0.29
irx2-1	8.77 ± 0.27
irx3	9.87 ± 0.28

[a] Samples are the mean of three to six samples ±SE.

To obtain a more quantitative analysis of the lignin content of the cell wall, we analyzed the phenolic content of stem cell walls by using the acetyl bromide method. The results showing total phenolics expressed as a percentage of the ethanol-insoluble wall material are shown in Table 1. No decrease in the phenolics content of the wall preparations was observed in any of the *irx* mutants (Table 1).

Carbohydrate Analysis of the Wall

The carbohydrate fraction of plant cell walls may be conveniently divided into a cellulose fraction, insoluble in weak acids, and a non-cellulose fraction. The non-cellulose carbohydrate fraction of the wall was examined by hydrolyzing the polysaccharides in weak acid, forming alditol acetates of the sugars, and separating the alditol acetates by gas chromatography (Blakeney et al., 1983; Reiter et al., 1993). Hypocotyls from mature plants proved to be a convenient tissue for this analysis because they contain a high proportion of xylem cells with heavily thickened secondary cell walls. Figure 8 shows the carbohydrate composition of a crude cell wall fraction from hypocotyls of mature plants. Only very small differences in the cell wall compositions between the wild-type and the *irx* plants were observed. All four lines showed a very high xylose content (~70%), which is characteristic of the composition of secondary cell walls from many angiosperms (Bacic et al., 1988). The relative proportions of sugars in hypocotyls (Figure 8) are quite different from the composition obtained from the walls of leaf tissues (Reiter et al., 1993), which do not contain a high proportion of cells with thick secondary cell walls. The sugar composition of cell walls from stems exhibited a composition very similar to hypocotyls, with xylose being the predominant sugar. No differences could be detected between the wild-type and the *irx* plants (data not shown).

Cellulose content in various tissues was measured by the method of Updegraff (1969), which has been used widely to measure cellulose in a number of plant species, including Arabidopsis (Potikha and Delmer, 1995). At all stages of stem development, all three *irx* mutants showed a large decrease in total cellulose content of the stem (Figure 9B). In stems from 36-day-old plants, all three *irx* mutants had <20% of the cellulose content of the wild type (Figure 9B). A similar pattern was observed if the amount of cellulose is expressed as a proportion of the ethanol-insoluble cell wall material (Figure 9A) as opposed to a "per stem" basis (Figure 9B). In wild-type plants, the proportion of cellulose increased during the course of stem development. In contrast, the mutants exhibited no increase in cellulose content during the same period, and in the case of *irx3*, there was actually a decrease in the proportion of cellulose in the wall (Figure 9A). Consequently, the differences in the proportion of cellulose between the wild type and mutants were greatest in older stems. In stems from 36-day-old plants, *irx1*, *irx2*, and *irx3* had 40, 36, and 18%, respectively, of the cellulose content of the wild type. During the period in which the cellulose analysis was conducted, the cells had ceased dividing and achieved their final size. Thus, the changes in cell wall composition are solely a consequence of secondary cell wall deposition.

Other tissues, such as mature hypocotyls, showed similarly large alterations in the cellulose content of the wall (Table 2). *irx1*, *irx 2*, and *irx3* had 40, 42, and 30%, respectively, of the cellulose content of the wild type (Table 2). In contrast, when the cellulose content of leaves was determined, the results showed very little difference between that of the mutant and the wild type. Only *irx1* showed a small but reproducible difference between the mutant and the wild type (Table 2). It is interesting that both mature stems and hypocotyls have a high proportion of cells with heavily thickened walls, whereas leaves contain only a small proportion of cells with heavily thickened, lignified cell walls. These data

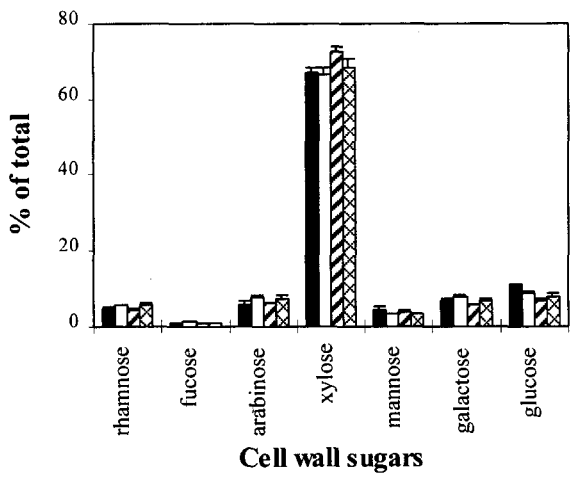

Figure 8. Cell Wall Composition of the Noncellulose Carbohydrate Fraction of Mature Hypocotyls from Wild-Type and *irx* Plants.

Individual sugars are expressed as a percentage of the total cell wall sugars and are shown for wild-type (solid bars), *irx1* (open bars), *irx2* (hatched bars), and *irx3* (cross-hatched bars) plants. Standard error bars are shown (n = 5).

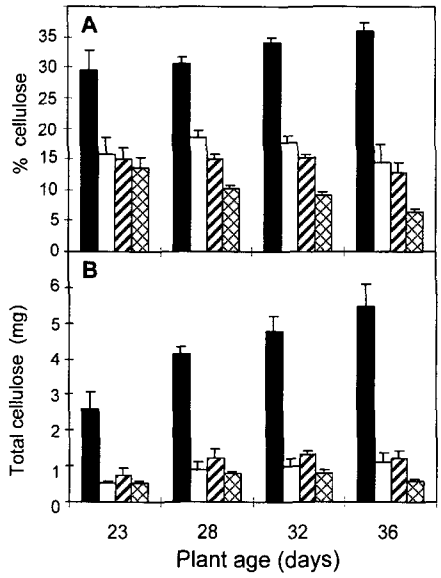

Figure 9. Cellulose Content of Developing Stems from Wild-Type and *irx* Plants.

Cellulose was measured in stem segments from wild-type (solid bars), *irx1* (open bars), *irx2* (hatched bars), and *irx3* (cross-hatched bars) plants. Standard error bars are shown ($n = 6$).

(A) Cellulose content expressed as a proportion of the ethanol-insoluble cell wall material.

(B) Cellulose content per 5-cm stem segment.

strongly suggest that the *irx* mutations primarily affect cellulose deposition in secondary cell walls.

DISCUSSION

During the course of xylem element differentiation, the cell walls are reinforced with an elaborate pattern of secondary cell wall thickening. This synthesis of a thick secondary wall by xylem elements is generally considered to be essential to allow these cells to withstand the negative pressures that are generated in the xylem during the course of water transport (Raven, 1977). Experiments in which bean seedlings were treated with the phenylalanine ammonia-lyase inhibitor aminooxyphenylpropionic acid (AOPP) graphically demonstrate the consequences of preventing the synthesis of an essential secondary cell wall component, such as lignin. Unable to withstand the negative pressure, the xylem elements in the epicotyls of these plants collapsed inward (Amrhein et al., 1983; Smart and Amrhein, 1985). The collapsed xylem phenotype of *irx* plants is similar in appearance to the xylem elements of the AOPP-treated plants. When viewed in cross-section, the xylem elements of *irx* plants do not have the normal round appearance but appear to be irregularly shaped and collapsed (Figure 3).

In common with the AOPP-treated plants, the xylem elements that are most distorted in *irx* plants are generally the early-forming protoxylem elements. These protoxylem elements have simple spiral or annular patterns of thickening in which the secondary thickening covers only a small proportion of the cell wall. In contrast, later-forming metaxylem elements have more elaborate reticulate or pitted patterns of thickening in which the secondary cell wall covers the majority of the wall. A smaller proportion of the cell wall is heavily thickened in protoxylem elements, which presumably makes them far less resistant than metaxylem elements to the negative pressures in the xylem.

If the collapse of the xylem cells in *irx* plants is due to the negative pressure of the xylem, it should only occur in cells that are actively transporting water. Indeed, no collapse has ever been observed in a xylem element that still contains its cellular contents and is therefore not involved in water transport. In addition, the xylem elements of *irx* plants initially expand normally and attain their proper shape (Figure 2). It is only after the cells die and lose their cell contents that the collapsed-cell phenotype is observed. Cells from the interfascicular region, which do not participate in water transport, retain normal shapes. Ultrastructural studies (Figure 6) clearly show that these cells have abnormal cell walls that appear to be deficient in secondary cell wall thickening. Considered together, these observation are consistent with the idea that the collapse of the xylem elements in *irx* mutants is due to the negative pressure generated in functioning xylem elements.

In addition to the collapsed-xylem phenotype, several independent lines of evidence indicate that the *irx* phenotype is the result of a cell wall defect. The physical properties of the stem, which reflect the properties of the cell wall (Kokubo et al., 1989, 1991), are radically altered. The stem material of *irx* plants is both weaker and much less stiff than that of the wild type (Figure 7). Ultrastructural analysis (Figure 6), which shows large alterations in the structure of secondary cell walls of *irx* plants, together with a specific decrease in cellulose in their cell walls (Figure 9), also supports this conclusion.

The cells of the xylem are only a minor proportion of the cells in the stem. Indeed, the sclerified parenchyma of the

Table 2. Percentage of Cellulose in an Ethanol-Insoluble Cell Wall Fraction from Fully Expanded Mature Leaves or Hypocotyls

Line	Hypocotyls[a] (% Cellulose)	Mature Leaves[a] (% Cellulose)
Landsberg *erecta*	36.1 ± 1.2	6.2 ± 0.74
irx1	14.4 ± 3.06	5.3 ± 0.23
irx2	13.0 ± 1.58	6.0 ± 0.24
irx3	6.4 ± 5.1	6.2 ± 0.27

[a] Values are the mean of measurements from six samples ±SE.

interfascicular region contains more cells with heavily thickened secondary cell walls (Figure 1). The alterations in both the physical properties of stems and cellulose content from *irx2* and *irx3* plants are large enough to suggest that it is not just the walls of the xylem cells that are affected but that the secondary cell walls from other cell types are also affected. This conclusion from physical studies is consistent with ultrastructural studies and the collapsed xylem phenotype. Together, these data suggest that the *irx* mutants are defective in some aspect of secondary cell wall biosynthesis. In the case of *irx2* and *irx3*, the defect appears to affect most if not all secondary cell walls in the stem. In contrast, the *irx1* mutant has the smallest alteration in cellulose content and physical properties of the stem and exhibits only small changes in the ultrastructure of the secondary walls of cells from the interfascicular region. However, the collapsed xylem phenotype of the *irx1* mutant is equally or more severe than that of the *irx2* or *irx3* mutants. These observations may be explained if the effects of *irx1* are normally limited to secondary cell walls of the xylem. *irx1* may therefore define a step in cellulose biosynthesis exclusive to the xylem.

The *irx* phenotype resembles that found in plants that have been treated with AOPP to reduce their lignin content (Smart and Amrhein, 1985). Consequently, initial experiments to determine the nature of the cell wall defects in the *irx* mutations focused on an analysis of the lignin fraction of the cell wall. Experiments using a range of histochemical methods, including staining with phloroglucinol (Figure 3) and measurement of total cell wall phenolics (Table 1), revealed no differences in lignin content between wild-type and *irx* lines. The method of lignin analysis used in these experiments provided no information about the structure of the lignin and conveys no information about degree of intersubunit subunit cross-linking. Thus, although the available evidence indicates that the *irx* phenotype is not due to a decrease in the amount of lignin, it does not preclude an alteration in the higher order structure of lignin in the walls of the mutants.

Analysis of the sugar composition of the noncellulosic fraction of stem cell walls from the mutants revealed no significant differences between wild-type and mutant lines (Figure 7). The high xylose content of the hypocotyl cell walls of *irx* plants, a characteristic of secondary cell walls, together with results of the lignin analysis suggest that the *irx* mutants still appear to deposit normal amounts of lignin and hemicellulose in the secondary cell wall. Thus, the *irx* mutations do not prevent the initiation of a secondary cell wall.

In contrast to the apparent lack of effect on lignin and noncellulose sugar composition, cellulose levels were strikingly reduced in the stems and hypocotyls of all three mutants when compared with those of the wild type. During stem maturation, the main site of cell wall synthesis is in the secondary cell wall. The differences in cellulose content between wild-type and *irx* stems increased during this same period. In addition, leaves contained a relatively low proportion of heavily thickened cells and did not show the same alterations in cellulose content (Table 2). This correlation, in which the largest difference in cellulose content between *irx* and the wild type occurs in tissues with a high proportion of cells with heavily thickened cell walls, suggests that the *irx* mutations specifically affect secondary cell wall cellulose deposition.

Only a fraction of the cells in the stem have heavily thickened lignified cell walls (Figure 1). The cellulose analysis was conducted with stem segments containing a large number of cells that did not undergo dramatic secondary thickening but still contained a substantial quantity of cellulose in the primary cell wall. This cellulose, present in the primary walls of these cells, may have caused the effect that the *irx* mutations had on the deposition of cellulose in secondary cell walls to be underestimated. This is generally consistent with the ultrastructural analysis, which suggests very large changes in cell wall composition (Figure 6). However, it is impossible to predict how alterations in cellulose content will affect the appearance of cell walls. The nature of the dark-staining outer regions in the walls of *irx3* plants (Figure 6D) is not known. One possibility is that these domains represent regions with a very high lignin content that arise because the normal locations of lignin deposition are missing or reduced in quantity.

There is a good correlation between cellulose content and the physical properties of the stem. *irx3* showed the greatest decrease in cellulose content, whereas *irx1* had the smallest decrease (Figure 9). This ranking also holds for the alterations in physical properties of the stem; *irx3* had the greatest alterations in physical properties and *irx1* had the smallest (Figure 7). In addition, the differences in the physical properties of the stem between the wild-type and the *irx* plants increased in stems of increasing age (Figure 7). A similar pattern was observed when differences in the cellulose content of the wall were determined (Figure 9), providing a good correlation between the cellulose content and physical properties of the stem. In addition, the high proportion of cellulose in the secondary cell wall and the unique structural properties of cellulose (Delmer and Amor, 1995) make it highly likely that it is the decrease in cellulose content of the wall that is responsible for both the collapse of the xylem elements and the alteration in the physical properties of the stem exhibited by *irx* lines.

In the *brittle culm* mutants of barley, there is a correlation between cellulose content and the maximum load at yield (Kokubo et al., 1989, 1991), and it is similar to that observed in this study. The *irx* mutations appear to affect the bending modulus more dramatically than the maximum load at yield. The effect of the *brittle culm* mutations on the bending modulus was not reported. In addition, the *brittle culm* mutants apparently do not show a collapsed-xylem phenotype, despite the decrease in cellulose content of the secondary cell wall. The reason for this is unclear, although it is possible that it may be a consequence of differences in the structure of monocot and dicot walls or that the *brittle culm* mutations may not affect the secondary cell walls of xylem elements.

In the generally accepted model for secondary cell walls, lignin is proposed to give the wall rigidity and resistance

to compressive forces (Wardrop, 1971). It is thought that whereas cellulose microfibrils are resistant to tensile forces, compressive forces would cause the microfibrils to buckle laterally unless lignin is packed between the fibrils (Frey-Wyssling, 1976). The fact that the xylem elements of *irx* plants collapse inward and that their stems show increased flexibility suggests that the walls of these lines are not resistant to compressive forces. Because *irx* plants appear to have normal levels of lignin, the question arises as to why, in the absence of normal cellulose levels, lignin alone apparently is unable to impart normal levels of rigidity on the wall.

The simplest explanation is that cellulose also contributes directly to the resistance of the wall to compressive forces. An alternative hypothesis arises from a proposal that the phenol rings of lignin are aligned in planes within the wall (Atalla and Agarwal, 1985). The mechanisms that lead to this proposed level of organization are not known. However, computational studies by Houtman and Atalla (1995) suggest that in secondary cell walls, the orientation of the lignin may be a consequence of its interaction with cellulose. Direct evidence that cellulose is required for normal lignin deposition was obtained by treating zinnia cells with 2,6-dichlorobenzonitrile to specifically inhibit cellulose biosynthesis during tracheary element differentiation. The treated cells exhibited an abnormal, dispersed pattern of lignin deposition (Taylor et al., 1992). Thus, the reduced levels of cellulose in the *irx* mutants may prevent normal deposition of lignin, and this lack of proper organization may have consequences for its pattern of cross-linking and/or the physical properties of the stem. A detailed analysis of lignin structure in the mutants by Raman spectroscopy or related analytical methods (Atalla and Agarwal, 1985) together with more detailed chemical analysis of lignin structure may be required to evaluate this possibility.

The similarity of the phenotypes exhibited by the three classes of *irx* mutants suggests that the three *irx* loci define different steps or components required for cellulose synthesis. They could encode regulatory proteins that are required to control the amount of cellulose, or perhaps they could encode components of a multisubunit complex that is required for normal cellulose deposition and orientation (Delmer and Amor, 1995). Relatively little is known about cellulose synthesis in higher plants (Delmer and Amor, 1995; Brown et al., 1996). By contrast, cellulose synthesis is now relatively well understood in some bacterial species (Ross et al., 1991). Four genes have been identified in the cellulose synthase operon of *Acetobacter xylinum* (Wong et al., 1990), and five genes have been identified as being required for cellulose synthesis in Agrobacterium (Matthysse et al., 1995). Only one gene, encoding the synthase subunit, shows homology between the two systems. This subunit corresponds to the family of cotton and Arabidopsis genes recently reported by Pear et al. (1996).

By analogy to bacterial systems, it is likely that several different gene products are required for cellulose synthesis in higher plants. In addition to a synthase subunit, genes encoding proteins required for the generation of UDP–glucose, passage of the cellulose chain through the membrane, and proper crystallization are also likely to be essential (Delmer and Amor, 1995). Higher plants also require that cellulose microfibrils be carefully orientated within both primary and secondary cell wall. Additional gene products are almost certainly required for this proper orientation and for the regulation of activity. The fact that cell wall deposition in *irx2* occurs preferentially in the corner of the cell suggests that the spatial deposition of cellulose in this mutant is not properly controlled. It is interesting that whereas *irx2* and *irx3* have similar affects on cell wall strength, *irx3* has a much greater affect on cell wall stiffness. The altered spatial pattern of cell wall distribution in *irx2* may explain these differences.

In summary, it is likely that the three *irx* mutants described here will serve as useful tools to probe secondary cell wall structure and function. In addition, the mutants should help to identify some of the genes involved in the synthesis and deposition of cellulose.

METHODS

Plant Material and Genetic Analysis

Arabidopsis thaliana plants were grown in controlled environment chambers under continuous illumination (140 to 220 mol m^{-2} sec^{-1}) at 23°C. Plant material used for physical and biochemical analysis was grown side by side.

Each mutant line has been assigned a name (e.g., SRT206-1) that refers unambiguously to the different backcross generations or the products of crosses. In some cases, the genotype of the lines is given parenthetically for convenience (e.g., SRT206-1 [*irx3*]). Line M53 (*gl1*), which was used as a parent in mapping experiments, was derived from the Columbia wild type by mutagenesis with ethlymethane sulfonate. Lines SRT123 (*irx1*), SRT228 (*irx2-1*), and SRT206 (*irx3*) were from a Landsberg *erecta* background, and line SRT177 (*irx2-2*) was isolated from the Columbia wild type, as described in the text. Most experiments were conducted with material that had been backcrossed once (SRT206-1) or twice (SRT123-2 and SRT228-2). No differences have been observed between lines crossed once and those that have been backcrossed four times (SRT123-4 and SRT228-4).

Mapping of *irx3* was performed by microscopically scoring the *irx* phenotype of 81 mutant plants from the F_2 generation of a cross between M53 and SRT206. Microsatellite markers were used as described by Bell and Ecker (1994). Map distances were calculated using the program Mapmaker 3.0 (Lander et al., 1987).

Microscopy

Stem sections ~200 μm in thickness were cut with a razor blade and stained in aqueous 0.02% toluidine blue O (Sigma) for 1 to 2 min, rinsed briefly in distilled water, and mounted in water. Alternatively, the sections were stained and mounted in phloroglucinol (saturated solution in 2 M HCl) and viewed immediately. Samples for transmission electron microscopy were fixed overnight in 4% formaldehyde, postfixed for 2 hr in 0.1 mg/mL osmium tetroxide, dehydrated in a graded series of alcohol (25, 50, 70, 90, 95, and 3 × 100% for at least

1 hr for each step), and embedded in Spurr's resin. Thin sections were cut with a diamond knife, stained in uranyl acetate and lead citrate, and viewed on an electron microscope (model 201; Philips, Cambridge, UK).

Physical Measurements

Segments (5 cm) cut from the base of the stems of 34- to 48-day-old plants were used immediately for three-point bending tests by using a universal testing machine (model 4301; Instron, High Wycombe, UK). A mean value for stem diameter was obtained by measuring the diameter at each end of the segment with a caliper. For bending tests, segments were placed on two supports separated by a distance of not less than 15 times the diameter (20 or 30 mm). A pushing probe with a 2-mm radius was then lowered until it was in contact with the stem. The crosshead was then lowered at 10 mm/min (Figure 10). Following a test, broken stem segments were frozen in liquid nitrogen before further biochemical analysis. At least 10 plants from each line were tested at every development stage. Maximum bending stress (λ_{max}, MPa) was calculated as $\lambda_{max} = F_{max}Lr/4I$, where F_{max} is the maximum force the sample will withstand before failure, L is the distance between the supports, r is the radius of the stem, and I is the second moment of the cross-sectional area of the stem ($r^4/4$). The bending rigidity (R) of a stem is the resistance of the beam to curvature and is given as $R = L^3 (dF/dY)/48$, where dF/dY is the initial slope of the force displacement curve (Figure 10). The bending modulus (MPa) is calculated as R/I (Gordon, 1978).

Carbohydrate Analysis

Analysis was conducted with material from a single plant by using three to five fully expanded leaves (from 28-day-old plants), the entire hypocotyl (from 36-day-old plants), or a 5-cm segment from the base of the primary inflorescence stem. Stems and hypocotyls were chopped with a razor blade, and a crude cell wall fraction was obtained by extracting the soluble material with two changes of 70% ethanol at 70°C for 1 hr each (Reiter et al., 1993). The ethanol was removed, the sample was dried under vacuum, and the dry weight of the wall material was recorded. The noncellulose fraction was analyzed according to the method of Blakeney et al. (1983). Essentially, the sugars were hydrolyzed by incubation in 2 M H_2SO_4 at 121°C for 1 hr, and then the alditol acetates of these sugars were analyzed by gas chromatography (Reiter et al., 1993). Cellulose was measured according to the method of Updegraff (1969). All noncellulose sugars were first hydrolyzed in acetic/nitric acid, and the cellulose content was then measured following swelling in 67% H_2SO_4. Measurements were repeated with two sets of independently grown plants by using at least five replicates for each developmental stage.

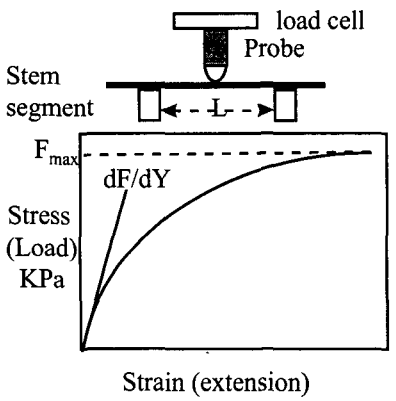

Figure 10. Measurement of the Physical Properties of an Arabidopsis Stem.

(Top) Diagrammatic representation of the setup used to measure the physical properties of Arabidopsis stem segments.
(Bottom) A typical stress-versus-strain curve obtained in such an experiment. KPa, kilopascals.

Lignin

Primary stem material (10 to 20 g) was harvested, frozen immediately in liquid nitrogen, and freeze dried. The material was extracted with 80% ethanol at 70°C for 1 hr to remove low molecular weight soluble sugars and soluble phenolic compounds, freeze dried, and finely ground under liquid nitrogen by using a freezer mill. Total cell wall phenolics were determined by the acetyl bromide method (Morrison, 1972), using ferulic acid as a standard.

ACKNOWLEDGMENTS

This work was supported by a grant from the U.S. Department of Energy (No. DE-FG02-94ER20133) and from the United Kingdom Biotechnology and Biological Sciences Research Council (No. 34/P06859). We gratefully acknowledge the help of Sandra Murison in measuring the cell wall phenolics, Roland Ennos for his advice on biomechanical studies, and Jo Ogas for his comments on the manuscript. In addition, we thank the staff of the Manchester University electron microscopy unit, particularly John Hutton and Sue Wilson, for help with the electron microscopy and Ian Miller for help with making the figures.

Received January 8, 1997; accepted March 3, 1997.

REFERENCES

Amrhein, N., Frank, G., Lemm, G., and Luhmann, H.B. (1983). Inhibition of lignin formation by L-alpha-aminooxy-beta-phenylpropionic acid, an inhibitor of phenylalanine ammonia-lyase. Eur. J. Cell Biol. **29,** 139–144.

Atalla, U.P., and Agarwal, R.H. (1985). Raman microprobe evidence for lignin orientation in the cell walls of native woody tissue. Science **227,** 636–638.

Bacic, A., Harris, P.J., and Stone, B.A. (1988). Structure and function of the plant cell wall. In The Biochemistry of Plants: A Comprehensive Treatise, Vol. 14, P.K. Stumpf and E.E. Conn, eds (New York: Academic Press), pp. 297–371.

Bell, C.J., and Ecker, J.R. (1994). Assignment of 30 microsatellite loci to the linkage map of Arabidopsis. Genomics **19,** 137–144.

Blakeney, N.B., Harris, P.J., Henry, R.J., and Stone, B.A. (1983). A simple and rapid preparation of alditol acetates for monosaccharide analysis. Carbohydr. Res. **182,** 291–299.

Brown, R.M., Saxena, I.M., and Kudlicka, K. (1996). Cellulose biosynthesis in higher plants. Trends Plant Sci. **1,** 149–156.

Carpita, N.C., and Gibeaut, D.M. (1993). Structural models of primary cell walls in flowering plants: Consistency of molecular structures with the physical properties of the walls during growth. Plant J. **3,** 1–30.

Delmer, D.P., and Amor, Y. (1995). Cellulose biosynthesis. Plant Cell **7,** 987–1000.

Frey-Wyssling, A. (1976). The Plant Cell Wall, 2nd ed. (Berlin: Borntraeger).

Fukada, H. (1992). Tracheary element formation as a model system for cell differentiation. Int. Rev. Cytol. **136,** 289–332.

Gordon, J.E. (1978). The Science of Strong Materials. (Middlesex, UK: Penguin).

Houtman, C.J., and Atalla, R.H. (1995). Cellulose–lignin interactions. A computational study. Plant Physiol. **107,** 977–984.

Kokubo, A., Kuraishi, S., and Sakurai, N. (1989). Culm strength of barley: Correlation among maximum bending stress, cell wall dimensions and cellulose content. Plant Physiol. **91,** 876–882.

Kokubo, A., Sakurai, N., Kuraishi, S., and Takeda, K. (1991). Culm brittleness of barley (*Hordeum vulgare* L.) mutants is caused by smaller number of cellulose molecules in cell wall. Plant Physiol. **97,** 509–514.

Lander, E., Green, P., Abrahamson, J., Barlow, A., Daly, M., Lincoln, S., and Newburg, L. (1987). MAPMAKER: An interactive computer package for constructing primary genetic linkage maps of experimental and natural populations. Genomics **1,** 174–181.

Lewis, N.G., and Yamamoto, E. (1990). Lignin occurrence biogenesis and biodegradation. Annu. Rev. Plant Physiol. Plant Mol. Biol. **41,** 455–496.

Matthysse, A.G., White, S., and Lightfoot, R. (1995). Genes required for cellulose synthesis in *Agrobacterium.* J. Bacteriol. **177,** 1069–1075.

McCann, M.C., and Roberts, K. (1994). Changes in cell wall architecture during cell elongation. J. Exp. Bot. **45,** 1683–1691.

McCann, M.C., Roberts, K., Wilson, R.H., Gidley, M.J., Gibeaut, D.M., Kim, J.-B., and Carpita, N.C. (1995). Old and new ways to probe plant cell-wall architecture. Can. J. Bot. **73,** S103–S113.

Morrison, I.M. (1972). A semi-micro method for the determination of lignin and its use in predicting the digestibility of forage crops. J. Sci. Food Agric. **23,** 455–463.

Pear, J.P., Kawagoe, Y., Schreckengost, W.E., Delmer, D.P., and Stalker, D.M. (1996). Higher plants contain homologs of the bacterial *celA* genes encoding the catalytic subunit of cellulose synthase. Proc. Natl. Acad. Sci. USA **93,** 12637–12642.

Potikha, T., and Delmer, D.P. (1995). A mutant of *Arabidopsis thaliana* displaying altered patterns of cellulose deposition. Plant J. **7,** 453–460.

Raven, J.A. (1977). The evolution of vascular plants in relation to supracellular transport processes. Adv. Bot. Res. **5,** 153–219.

Reiter, W.D. (1994). Structure, synthesis and function of the plant cell wall. In Arabidopsis, E. Meyerowitz and C.R. Somerville, eds (Cold Spring Harbor, NY: Cold Spring Harbor Laboratory Press), pp. 955–988.

Reiter, W.D., Chapple, C., and Somerville, C.R. (1993). Altered growth and development in a fucose-deficient cell wall mutant of *Arabidopsis.* Science **261,** 1032–1035.

Ross, P., Mayer, R., and Benzimen, M. (1991). Cellulose biosynthesis and function in bacteria. Microbiol. Rev. **55,** 35–58.

Shackel, K. (1996). To tense, or not to tense: Reopening the debate about water ascent in plants. Trends Plant Sci. **1,** 105–106.

Smart, C.C., and Amrhein, N. (1985). The influence of lignification on the development of vascular tissue in *Vigna radiata* L. Protoplasma **124,** 87–95.

Somerville, S., and Somerville, C. (1996). Arabidopsis at 7: Still growing like a weed. Plant Cell **8,** 1917–1933.

Taylor, G.J., Owen, T.P., Koonce, L.T., and Haigler, C.H. (1992). Dispersed lignin in tracheary elements treated with cellulose synthesis inhibitors provides evidence that molecules of the secondary cell wall mediate wall patterning. Plant J. **2,** 959–970.

Updegraff, D.M. (1969). Semi-micro determination of cellulose in biological materials. Anal. Biochem. **32,** 420–424.

Wardrop, A.B. (1971). Occurrence and formation in plants. In Lignins: Occurrence, Formation, Structure and Formation, K.V. Sarkanen and C.H. Ludwig, eds (New York: Wiley Interscience), pp. 19–41.

Whetten, R., and Sederoff, R. (1995). Lignin biosynthesis. Plant Cell **7,** 1001–1013.

Wong, H.C., Fear, A.L., Calhoon, R.D., Eichinger, G.H., Mayer, R., Amikam, D., Benziman, M., Gelfand, D.H., Meade, J.H., Emerick, A.W., Bruner, R., Ben-Basat, B.A., and Tal, R. (1990). Genetic organization of the cellulose synthase operon in *Acetobacter xylinum.* Proc. Natl. Acad. Sci. USA **87,** 8130–8134.

Zablackis, E., Huang, J., Muller, B., Darvill, A.G., and Albersheim, P. (1995). Characterization of the cell-wall polysaccharides of *Arabidopsis thaliana* leaves. Plant Physiol. **107,**1129–1138.

Zimmerman, U., Meinzer, F.C., Benkert, R., Zhu, J.J., Schneider, H., Goldstein, G., Kuchenbrod, E., and Haase, A. (1994). Xylem water transport: Is the available evidence consistent with the cohesion theory? Plant Cell Environ. **17,** 1169–1181.